Holographic nucleons in the nuclear medium

Bum-Hoon Lee [a,b], Chanyong Park [b,*]

[a] *Department of Physics, Sogang University, Seoul 121-742, Republic of Korea*
[b] *Center for Quantum Spacetime (CQUeST), Sogang University, Seoul 121-742, Republic of Korea*

ABSTRACT

We investigate the nucleon's rest mass and dispersion relation in the nuclear medium which is holographically described by the thermal charged AdS geometry. With this background, the chiral condensate plays an important role to determine the nucleon's mass in both the vacuum and the nuclear medium. It also significantly modifies the nucleon's dispersion relation. The nucleon's mass in the high density regime increases with density as expected, while in the low density regime it slightly decreases. We further study the splitting of the nucleon's energies caused by the isospin interaction with the nuclear medium.

© 2015 The Authors. Published by Elsevier B.V. This is an open access article under the CC BY license (http://creativecommons.org/licenses/by/4.0/). Funded by SCOAP³.

1. Introduction

The AdS/CFT correspondence is a fascinating and useful tool to understand physical phenomena. It says that the quantum field theory (QFT) in the strong coupling regime can be figured out from a classical one-dimensional higher gravity theory [1–4]. Many interesting phenomena of the quantum chromodynamics (QCD) and condensed matter theory happen in the strong coupling regime. Therefore, applying the AdS/CFT correspondence to them may shed light on understanding the nonperturbative aspects of various strongly interacting QFT [5–7].

In the QCD and its holographic models, there exists a deconfinement phase transition between hadrons and quarks [8–12]. Hadrons are fundamental excitations in the confining phase which usually reside in the strong coupling regime. In a nuclear medium, this confining phase transits into the deconfining phase above a certain critical temperature and chemical potential where hadrons dissolve into quarks [13–15,17]. In the holographic QCD model, the deconfinement phase transition is identified with the Hawking–Page transition of the dual gravity [16]. In this procedure, the deconfining phase maps to a black hole geometry, while the confining phase corresponds to a non-black-hole geometry with an appropriate IR modification [8–10]. In the hard wall model, the thermal AdS (tAdS) space with an IR cutoff corresponds to the confining phase without a nuclear density. If turning on a nonzero nuclear density, the dual geometry of the confining phase is gener-

alized to the tAdS with a nonzero electric charge which describes the flavor charge of the dual QCD [18–26]. This geometry was called the thermal charged AdS (tcAdS) space [21]. This geometry has a singularity at the center. However, in the hard wall model we need to introduce an IR cutoff in order to represent the confinement which prevents all bulk fields from approaching this singularity. Therefore, the singularity of tcAdS is not harmful at least in the hard wall model. On this tcAdS background the holographic study on the deconfinement phase transition have shown that the holographic phase diagram is similar to the one expected in particle phenomenology [15,21].

The holographic analysis on the tcAdS space has been further generalized to the case with two flavor charges by regarding $U(2)$ non-Abelian gauge fields [27–29]. In this case, the diagonal time components of these gauge fields are dual to the number density operators of proton and neutron, so one can interpreted a tcAdS geometry as a nuclear medium in the dual QFT. On this tcAdS space with two flavor symmetries, it was shown that the deconfinement phase transition and symmetric energy depend on the number asymmetry between proton and neutron [27]. Furthermore, the meson spectra represented by off-diagonal components of gauge fields were also studied [28,29]. In general, meson's masses increase with the density of the nuclear medium. On the other hand, the isospin interaction reduces the meson mass when the isospin charge of meson is opposite to the net isospin charge of nuclear medium. It was also shown that the competition between those two interactions can lead to the pion condensation in the high density regime [28,30–32].

Similarly, the nucleon's mass spectra have been investigated in the vacuum corresponding to tAdS [33–38] and further in the

isospin medium [39] which includes only the isospin chemical potential without the nuclear density effect. In general, there exist two different descriptions for baryons. The first is a Skyrmion model in which baryons can be understood as a solitonic object composed of pions. In [11,12], it has been shown that the Skyrmion-like solutions naturally appear in the top-down model with D4–D8 branes. The other is to introduce bulk fermions dual to baryons. The latter mimics the chiral perturbation theory and is useful to investigate various interactions between mesons and baryons. In this work, we will focus on the latter to study the medium effect on the nucleon's dispersion relation. Although the isospin medium provides a good playground to figure out the isospin effect on nucleon's masses, it is less physical. In order to understand more realistic nuclear physics phenomena, we need to go beyond the isospin medium. In this letter, we will holographically investigate nucleon's spectra in the nuclear medium composed of protons and neutrons.

The rest of paper is organized as follows. In Section 2, we summarize the tcAdS geometry with two flavor symmetries and explain how five-dimensional fermions living in tcAdS are reduced to proton and neutron in the dual QFT. In Section 3, we discuss nucleon's rest masses and dispersion relations in the nuclear medium. We finish this work with some concluding remarks in Section 4.

2. Nucleons in a nuclear medium

The nuclear matter is composed of two kinds of particles, proton and neutron, with the baryon and isospin charges. In order to describe it holographically, one should take into account a gravity theory including at least $U(2)$ flavor symmetry. Here we regard an $U(2)_L \times U(2)_R$ flavor group to represent parity explicitly. In the dual QFT, it is related to the chirality of nucleons [33,40–43]. In the hard wall model, the gravity action describing the holographic nuclear medium is given by [28,29]

$$S = \int d^5 x \sqrt{-G} \left[\frac{1}{2\kappa^2} \left(\mathcal{R} - 2\Lambda \right) \right.$$
$$\left. - \frac{1}{4g^2} \left(F_{MN}^{(L)} F^{(L)MN} + F_{MN}^{(R)} F^{(R)MN} \right) \right], \quad (1)$$

where $\Lambda = -6/R^2$ is the cosmological constant and the gauge field strengths for $U(2)_L$ and $U(2)_R$ are given by

$$F_{MN}^{(L)} = \partial_M L_N - \partial_N L_M - i [L_M, L_N],$$
$$F_{MN}^{(R)} = \partial_M R_N - \partial_N R_M - i [R_M, R_N]. \quad (2)$$

The nuclear medium can be classified by two quantum numbers, baryon and isospin charges [27]. This fact implies that it is sufficient to turn on only diagonal time components of the gauge field because they uniquely determine quantum numbers of the nuclear medium. Their nontrivial values, V_t^0 and V_t^3, break the $U(2)_L \times U(2)_R$ flavor group to $U(1)_L^2 \times U(1)_R^2$. This reduced flavor symmetry group can be further decomposed into the symmetric and anti-symmetric combinations, $U(1)_S^2$ and $U(1)_A^2$. In this case, the symmetric combination corresponds to a parity-even state, while the antisymmetric one describes a parity-odd state. The lowest parity-even states are identified with proton and neutron. Since the energy of a parity-even state is lower than that of a parity-odd state, it is natural in the low energy regime to consider a nuclear medium composed of the lowest parity-even states [33, 39]. In the holographic model, it can be accomplished by taking

$L_M = R_M = -V_M.$[1] On this background, the deconfinement phase transition and the symmetry energy have been studied in [27]. In additions, $SU(2)$ meson spectra have been investigated in [28].

In the holographic model, the dual operators of V_t^0 and V_t^3 correspond to baryon and isospin charge of quark respectively. To see this, let us recall the AdS/CFT correspondence. The dual operator of the bulk gauge field should have the conformal dimension 3. One of candidates is a fermionic current, $\bar{\psi} \gamma_\mu \psi$, because a fermionic field in a $(3+1)$-dimensional conformal field theory has a conformal dimension $3/2$. This fact indicates that the duals of the bulk gauge fields are not nucleons but quarks. However, since fundamental excitations in the confining phase are nucleons, one need to reinterpret quark's quantum numbers in terms of nucleon's quantities. In the hard wall model representing the confining phase, these quark's quantities can be easily reinterpreted as nucleon's ones by using the conservation of the net quark number. As a consequence, the resulting tcAdS geometry can be described by [27,28]

$$ds^2 = \frac{R^2}{z^2} \left(-f(z) dt^2 + \frac{1}{f(z)} dz^2 + d\vec{x}^2 \right), \quad (4)$$

with

$$f(z) = 1 + \frac{3Q^2 \kappa^2}{g^2 R^2} z^6 + \frac{D^2 \kappa^2}{3g^2 R^2} z^6,$$
$$V_t^0 = \frac{Q}{\sqrt{2}} \left(2z_{\mathrm{IR}}^2 - 3z^2 \right),$$
$$V_t^3 = \frac{D}{3\sqrt{2}} \left(2z_{\mathrm{IR}}^2 - 3z^2 \right), \quad (5)$$

where $Q = Q_P + Q_N$ and $D = Q_P - Q_N$ denote the total nucleon number density and density difference between proton and neutron. Here Q_p and Q_N are the number of proton and neutron respectively.

In the confining phase, another important ingredient is the chiral condensate. In order to see the chiral condensate effect, one should further introduce a complex scalar field Φ with a negative mass, $-3/R^2$. Let us parameterize the complex scalar field as

$$\Phi = \phi \mathbb{1} e^{i\sqrt{2}\pi}, \quad (6)$$

where $\pi = \pi^i T^i$ with the $SU(2)$ generators, T^i. Then, the modulus ϕ can be mapped to the chiral condensate, while π^i corresponds to the pseudoscalar fluctuations, the so-called pions. From now on, we set $R = 1$ for convenience. On the geometry in (4) the modulus ϕ satisfies the following equation of motion [28]

$$0 = \frac{1}{\sqrt{-g}} \partial_z \left(\sqrt{-g} g^{zz} \partial_z \phi \right) + 3\phi, \quad (7)$$

and its solution is given by

$$\phi(z) = m_q z \, {}_2F_1 \left(\frac{1}{6}, \frac{1}{2}, \frac{2}{3}, -\frac{(D^2 + 9Q^2) z^6}{3N_c} \right)$$
$$+ \sigma z^3 \, {}_2F_1 \left(\frac{1}{2}, \frac{5}{6}, \frac{4}{3}, -\frac{(D^2 + 9Q^2) z^6}{3N_c} \right), \quad (8)$$

---

[1] This convention is different from the one used in [28]. However, the results in [28] can be reproduced by defining mesons differently. For example, defining charged ρ-mesons like

$$\rho_m^\pm = \frac{1}{\sqrt{2}} \left(v_m^1 \mp i v_m^2 \right), \quad (3)$$

reproduces the same meson mass spectrum obtained in [28].

where m_q and σ denote the current quark mass and chiral condensate respectively and N_c is the rank of the gauge group. In general, the gravitational backreaction of the scalar field changes the background geometry. As shown in [44], it corresponds to $1/N_c$ correction. In this letter we ignore the gravitational backreaction of the scalar field, as done in usual holographic models [8–10].

The tcAdS geometry, as explained before, is dual to a nuclear medium composed of the lowest parity-even states, proton and neutron. In order to describe nucleons in this nuclear medium, we should introduce corresponding bulk fields on this tcAdS space. Since nucleons are fermions, the corresponding bulk fields should be also fermions. Then, bulk fermions in the tcAdS background are governed by [33,36–39]

$$
S = i \int d^5 x \sqrt{-G} \Big[\overline{\Psi}^1 \Gamma^M \nabla_M \Psi^1 + \overline{\Psi}^2 \Gamma^M \nabla_M \Psi^2
$$
$$
- m_1 \overline{\Psi}^1 \Psi^1 - m_2 \overline{\Psi}^2 \Psi^2
$$
$$
- g_Y \left(\overline{\Psi}^1 \Phi \Psi^2 + \overline{\Psi}^2 \Phi^+ \Psi^1 \right) \Big],
\tag{9}
$$

where g_Y denotes the Yukawa coupling. Since we are interest in nucleons rather than quarks in the confining phase, the mass of bulk fermions must be $\pm 5/2$ because this value is related to the conformal dimension of nucleons, $9/2$, in the dual field theory. Here, we do not take into account the anomalous dimension for simplicity. If regarding the anomalous dimension, the baryon operator can have a smaller conformal dimension and its physical properties can be affected by the conformal dimension change. We leave this issue as a future work.

In order to realize the chirality of the 4-dimensional fermions from the 5-dimensional parity under $U(2)_L \leftrightarrow U(2)_R$, we take $m_1 = -m_2 = 5/2$. Above the covariant derivative ∇_M is defined as

$$
\nabla_M \Psi^1 = \left(\partial_M - \frac{i}{4} \omega_M - i L_M \right) \Psi^1,
$$
$$
\nabla_M \Psi^2 = \left(\partial_M - \frac{i}{4} \omega_M - i R_M \right) \Psi^2.
\tag{10}
$$

In this case, Ψ^1 and Ψ^2 transform as $\left(\frac{1}{2}, 0 \right)$ and $\left(0, \frac{1}{2} \right)$ under the flavor group. In general, the Yukawa term couples Ψ^1 to Ψ^2 and then breaks the chiral symmetry.

The variation of action leads to the following Dirac equations

$$
0 = \left[e_C^M \Gamma^C \left(\partial_M - \frac{i}{4} \omega_M^{AB} \Gamma_{AB} + i V_M \right) - m_1 \right] \Psi^1 - g_Y \phi \Psi^2,
$$
$$
0 = \left[e_C^M \Gamma^C \left(\partial_M - \frac{i}{4} \omega_M^{AB} \Gamma_{AB} + i V_M \right) - m_2 \right] \Psi^2 - g_Y \phi \Psi^1,
\tag{11}
$$

where $\Gamma^{AB} = \frac{i}{2} \left[\Gamma^A, \Gamma^B \right]$ and $L_M = R_M = -V_M$ is used. For the well-defined variation, the solutions of the Dirac equations should satisfy the following boundary condition

$$
\delta \overline{\Psi}^{(1,2)} \Gamma^M \Psi^{(1,2)} \Big|_{\epsilon}^{z_{IR}} = 0,
\tag{12}
$$

where z_{IR} and ϵ are the IR and UV cutoff respectively. Since this Dirac equation is defined on the curved manifold, it is more convenient to introduce quantities on the tangent manifold. The vielbein e_M^A of the tcAdS space is given by

$$
e_M^A = \text{diag} \left(\frac{\sqrt{f(z)}}{z}, \frac{1}{z}, \frac{1}{z}, \frac{1}{z}, \frac{1}{z\sqrt{f(z)}} \right),
\tag{13}
$$

where A, B and M, N are indices of the tangent and curved manifold respectively. Then, non-zero components of spin connection ω_M^{AB} are given by

$$
\omega_M^{5A} = \text{diag} \left(\frac{f(z)}{z} - \frac{f(z)'}{2}, \frac{\sqrt{f(z)}}{z}, \frac{\sqrt{f(z)}}{z}, \frac{\sqrt{f(z)}}{z}, 0 \right).
\tag{14}
$$

We choose the following gamma matrices on the tangent space

$$
\Gamma^0 = \begin{pmatrix} 0 & i \\ i & 0 \end{pmatrix}, \quad \Gamma^i = \begin{pmatrix} 0 & -i\sigma^i \\ i\sigma^i & 0 \end{pmatrix}, \quad \Gamma^4 = \begin{pmatrix} 1 & 0 \\ 0 & -1 \end{pmatrix}.
\tag{15}
$$

Since Γ^0 is pure imaginary, $\overline{\Psi}\Psi$ is not invariant under the hermitian conjugation. To make the action invariant under the hermitian conjugation, i in front of the fermion action was inserted. If one further defines the 4-dimensional gamma matrices $\gamma^\mu = \Gamma^\mu$ ($\mu = 0, 1, 2, 3$), then the 4-dimensional chirality operator is given by $\gamma^5 = \Gamma^4$.

Now, let us think of the Fourier mode expansion of 5-dimensional fermions

$$
\Psi(z, t, \vec{x}) = \sum_{\omega_n} \int \frac{d^3 p}{(2\pi)^4} \, \Psi(z, \omega_n, \vec{p}) \, e^{-i(\omega_n t - \vec{p} \cdot \vec{x})},
\tag{16}
$$

where Ψ implies either Ψ^1 or Ψ^2. Since solutions of 5-dimensional Dirac equations usually depend on the parity and isospin charge it is useful to represent fermions with the parity and isospin quantum numbers. In terms of 4-dimensional Weyl spinors, ψ_L and ψ_R satisfying $\psi_L = \gamma^5 \psi_L$ and $\psi_R = -\gamma^5 \psi_R$, the Fourier mode can be further decomposed into [39]

$$
\Psi^1(z, \omega_n, \vec{p}) = \begin{pmatrix} f_L^{1(n,\pm,\pm)} \psi_L^{(n,\pm,\pm)} \\ f_R^{1(n,\pm,\pm)} \psi_R^{(n,\pm,\pm)} \end{pmatrix} \quad \text{and}
$$
$$
\Psi^2(z, \omega_n, \vec{p}) = \begin{pmatrix} f_L^{2(n,\pm,\pm)} \psi_L^{(n,\pm,\pm)} \\ f_R^{2(n,\pm,\pm)} \psi_R^{(n,\pm,\pm)} \end{pmatrix},
\tag{17}
$$

where n denotes the n-th resonance and the first and second sign imply the parity and isospin quantum number respectively. In these decompositions, the mode functions denoted by $f_{L,R}^{1,2}$ are given by functions of z, ω_n and $\vec{p}$.

If one takes the normalizable mode functions to be f_L^1 and f_R^2, the 5-dimensional parity under the $U(2)_L \times U(2)_R$ flavor group can be associated with the 4-dimensional chirality. Using the previous Fourier mode decomposition, the 5-dimensional Dirac equations in (11) are reduced to

$$
\begin{pmatrix} \mathcal{D}_- \mathbb{1} & -\frac{g_Y \phi}{z} \mathbb{1} \\ -\frac{g_Y \phi}{z} \mathbb{1} & \mathcal{D}_+ \mathbb{1} \end{pmatrix} \begin{pmatrix} f_L^{1(n,\pm,\pm)} \\ f_L^{2(n,\pm,\pm)} \end{pmatrix}
$$
$$
= -\begin{pmatrix} \mathbb{E}_+ & 0 \\ 0 & \mathbb{E}_+ \end{pmatrix} \begin{pmatrix} f_R^{1(n,\pm,\pm)} \\ f_R^{2(n,\pm,\pm)} \end{pmatrix},
\tag{18}
$$
$$
\begin{pmatrix} \mathcal{D}_+ \mathbb{1} & \frac{g_Y \phi}{z} \mathbb{1} \\ \frac{g_Y \phi}{z} \mathbb{1} & \mathcal{D}_- \mathbb{1} \end{pmatrix} \begin{pmatrix} f_R^{1(n,\pm,\pm)} \\ f_R^{2(n,\pm,\pm)} \end{pmatrix}
$$
$$
= \begin{pmatrix} \mathbb{E}_- & 0 \\ 0 & \mathbb{E}_- \end{pmatrix} \begin{pmatrix} f_L^{1(n,\pm,\pm)} \\ f_L^{2(n,\pm,\pm)} \end{pmatrix},
\tag{19}
$$

where $\mathbb{1}$ denotes a 2×2 identity matrix and

$$
\mathcal{D}_\pm = \sqrt{f(z)} \left[\partial_z - \frac{2}{z} \left(1 - \frac{zf'}{8f(z)} \right) \right] \pm \frac{5}{2z},
\tag{20}
$$

$$
\mathbb{E}_\pm = \frac{1}{\sqrt{f(z)}} (\omega_n - V_t) \, \mathbb{1} \pm \vec{\sigma} \cdot \vec{p} \, .
\tag{21}
$$

Above most matrix elements are proportional to the identity matrix except the last term in (21). To solve the Dirac equation, we first need to determine mode functions as eigenfunctions of $\vec{\sigma} \cdot \vec{p}$. By using the rotation symmetry, without loss of generality, we can take the momentum vector to be $\vec{p} = \{0, 0, \pm p\}$. In this case, mode functions are identified with momentum eigenfunctions with an eigenvalue, p or $-p$. Now, we take f_L^1 and f_R^1 to be eigenfunctions

with the eigenvalue p and f_L^2 and f_R^2 as eigenfunctions with $-p$. Then, (18) and (19) are further simplified to

$$
\begin{pmatrix} \mathcal{D}_- \mathbb{1} & -\frac{g_Y \phi}{z} \mathbb{1} \\ -\frac{g_Y \phi}{z} \mathbb{1} & \mathcal{D}_+ \mathbb{1} \end{pmatrix} \begin{pmatrix} f_L^{1(n,\pm,\pm)} \\ f_L^{2(n,\pm,\pm)} \end{pmatrix}
$$
$$
= - \begin{pmatrix} E_+ \mathbb{1} & 0 \\ 0 & E_- \mathbb{1} \end{pmatrix} \begin{pmatrix} f_R^{1(n,\pm,\pm)} \\ f_R^{2(n,\pm,\pm)} \end{pmatrix}, \tag{22}
$$

$$
\begin{pmatrix} \mathcal{D}_+ \mathbb{1} & \frac{g_Y \phi}{z} \mathbb{1} \\ \frac{g_Y \phi}{z} \mathbb{1} & \mathcal{D}_- \mathbb{1} \end{pmatrix} \begin{pmatrix} f_R^{1(n,\pm,\pm)} \\ f_R^{2(n,\pm,\pm)} \end{pmatrix}
$$
$$
= \begin{pmatrix} E_- \mathbb{1} & 0 \\ 0 & E_+ \mathbb{1} \end{pmatrix} \begin{pmatrix} f_L^{1(n,\pm,\pm)} \\ f_L^{2(n,\pm,\pm)} \end{pmatrix}, \tag{23}
$$

with

$$
E_\pm = \frac{1}{\sqrt{f(z)}} (\omega_n - V_t) \pm p . \tag{24}
$$

In order to identify bulk fermionic components with nucleons of the dual QFT, let us introduce symmetric or antisymmetric combinations of mode functions. Defining the symmetric combination [33,36,38,39]

$$
f_L^{1(n,+,\pm)} = f_R^{2(n,+,\pm)} \quad \text{and} \quad f_R^{1(n,+,\pm)} = -f_L^{2(n,+,\pm)}, \tag{25}
$$

it describes a parity-even state. Inserting this symmetric relation into (22) and (23), one can easily check that (22) and (23) are reduced to the same matrix equation

$$
\begin{pmatrix} \mathcal{D}_- \mathbb{1} & \frac{g_Y \phi}{z} \mathbb{1} \\ \frac{g_Y \phi}{z} \mathbb{1} & \mathcal{D}_+ \mathbb{1} \end{pmatrix} \begin{pmatrix} f_L^{1(n,+,\pm)} \\ f_R^{1(n,+,\pm)} \end{pmatrix}
$$
$$
= \begin{pmatrix} -E_+ & 0 \\ 0 & E_- \end{pmatrix} \begin{pmatrix} f_R^{1(n,+,\pm)} \\ f_L^{1(n,+,\pm)} \end{pmatrix}. \tag{26}
$$

For a parity-odd state, we take an antisymmetric combination satisfying

$$
f_L^{1(n,-,\pm)} = -f_R^{2(n,-,\pm)} \quad \text{and} \quad f_R^{1(n,-,\pm)} = f_L^{2(n,-,\pm)}. \tag{27}
$$

Then, similar to the parity-even case (22) and (23) reach to

$$
\begin{pmatrix} \mathcal{D}_- \mathbb{1} & -\frac{g_Y \phi}{z} \mathbb{1} \\ -\frac{g_Y \phi}{z} \mathbb{1} & \mathcal{D}_+ \mathbb{1} \end{pmatrix} \begin{pmatrix} f_L^{1(n,-,\pm)} \\ f_R^{1(n,-,\pm)} \end{pmatrix}
$$
$$
= \begin{pmatrix} -E_+ & 0 \\ 0 & E_- \end{pmatrix} \begin{pmatrix} f_R^{1(n,-,\pm)} \\ f_L^{1(n,-,\pm)} \end{pmatrix}. \tag{28}
$$

The parity-even state has lower energy than the parity-odd state. In the QCD proton and neutron correspond to the lowest parity-even states. From now on, we concentrate on the lowest resonance with $n = 1$. In this case, mode functions, $f_{L,R}^{1(1,+,+)}$ and $f_{L,R}^{1(1,+,-)}$, represent proton and neutron respectively. Due to the different isospin charge of nucleons, the equation in (26) can be further splitted into two cases. Proton with the isospin charge $1/2$ is governed by

$$
\begin{pmatrix} \mathcal{D}_- \mathbb{1} & \frac{g_Y \phi}{z} \mathbb{1} \\ \frac{g_Y \phi}{z} \mathbb{1} & \mathcal{D}_+ \mathbb{1} \end{pmatrix} \begin{pmatrix} f_L^{1(1,+,+)} \\ f_R^{1(1,+,+)} \end{pmatrix}
$$
$$
= \begin{pmatrix} -\left\{ \frac{1}{\sqrt{f(z)}} \left(\omega - \frac{V_t^0 + V_t^3}{2} \right) + p \right\} & 0 \\ 0 & \frac{1}{\sqrt{f(z)}} \left(\omega - \frac{V_t^0 + V_t^3}{2} \right) - p \end{pmatrix}
$$
$$
\times \begin{pmatrix} f_R^{1(1,+,+)} \\ f_L^{1(1,+,+)} \end{pmatrix}, \tag{29}
$$

while for neutron with the isospin charge of $-1/2$ (26) yields

$$
\begin{pmatrix} \mathcal{D}_- \mathbb{1} & \frac{g_Y \phi}{z} \mathbb{1} \\ \frac{g_Y \phi}{z} \mathbb{1} & \mathcal{D}_+ \mathbb{1} \end{pmatrix} \begin{pmatrix} f_L^{1(1,+,-)} \\ f_R^{1(1,+,-)} \end{pmatrix}
$$
$$
= \begin{pmatrix} -\left\{ \frac{1}{\sqrt{f(z)}} \left(\omega - \frac{V_t^0 - V_t^3}{2} \right) + p \right\} & 0 \\ 0 & \frac{1}{\sqrt{f(z)}} \left(\omega - \frac{V_t^0 - V_t^3}{2} \right) - p \end{pmatrix}
$$
$$
\times \begin{pmatrix} f_R^{1(1,+,-)} \\ f_L^{1(1,+,-)} \end{pmatrix}, \tag{30}
$$

where we use $\omega = \omega_1$ for simplicity. Taking $V_t^0 = 0$, $V_t^3 = \text{const}$ and $f(z) = 1$, above equations reduces to those for nucleons in the isospin medium [39]. In the nuclear medium, unlike the isospin medium, the energy and mass crucially depends on the medium because of the nontrivial radial coordinate dependence in the metric and background gauge fields.

3. Nucleon spectrum in the nuclear medium

At given Q, D, m_q and σ, the energy and momentum of nucleons can be determined by solving (29) or (30) together with appropriate two boundary conditions. For the well-defined variation of the fermionic action, (12) should vanish. To do so, we impose the following two boundary conditions

$$
f_L^{1(n,\pm,\pm)}(0) = 0 \quad \text{and} \quad f_R^{1(n,\pm,\pm)}(z_{\text{IR}}) = 0, \tag{31}
$$

which was also used in studying the nucleon mass in the vacuum and isospin medium [33,39]. In general, solving the Dirac equation with above boundary conditions gives rise to a relation between parameters. Inversely, this fact implies that there exists a solution only in the case satisfying a specific parameter relation. Furthermore, since the range of z is restricted to $0 \le z \le z_{\text{IR}}$ in the hard wall model, the solution of the Dirac equation has a discrete eigenvalues. This is why we take a discrete energy values, ω_n, rather than continuous ones in the previous Fourier mode decomposition. As a consequence, the parameter relation obtained by solving the Dirac equation is nothing but the dispersion relation of nucleon because it expresses a discrete energy as a function of the other quantities. In this case, the rest mass of nucleon appears in the $p = 0$ limit. In general, the dispersion relation crucially depends on properties of the nuclear medium, Q and D. In this section, we will investigate how the nucleon's dispersion relation changes in the nuclear medium.

3.1. Dispersion relation in the vacuum

Before studying the nucleon's spectra in the medium, let's first consider the vacuum with $Q = D = 0$ in order to get more intuitions. In this case, the dual geometry is given by a tAdS space and proton and neutron become degenerate. If we further set $m_q = \sigma = 0$, the lowest nucleons with the energy ω are governed by

$$
\bar{\mathcal{D}}_+ \bar{\mathcal{D}}_- f_L^1 = -(\omega^2 - p^2) f_L^1,
$$
$$
\bar{\mathcal{D}}_- \bar{\mathcal{D}}_+ f_R^1 = -(\omega^2 - p^2) f_R^1, \tag{32}
$$

where $\bar{\mathcal{D}}_+ = \partial_z + \frac{1}{2z}$ and $\bar{\mathcal{D}}_- = \partial_z - \frac{9}{2z}$. Solutions of these equations depend only the value of $\omega^2 - p^2$. Suppose that there exists a solution at a given value of $\sqrt{\omega^2 - p^2}$. Denoting this value by $m_0 = \sqrt{\omega^2 - p^2}$, m_0 determines the nucleon's dispersion relation uniquely. In this case, nucleons follow the relativistic dispersion relation

$$
\omega^2 = m_0^2 + p^2. \tag{33}
$$

Since ω reduces to m_0 at $p = 0$, m_0 can be identified with the nucleon's rest mass. This relativistic dispersion relation is expected from the asymptotic symmetry of the tAdS geometry. Since the boundary space of tAdS is invariant under boundary Poincare symmetry, nucleons defined on this boundary should satisfy the relativistic dispersion relation. To check this, we numerically solve (32) for $m_q = \sigma = Q = D = 0$. Numerical results for the nucleon's energy are plotted in Fig. 1(a). The resulting curve is well fitted by the following dispersion relation

$$\omega = \sqrt{2.0589^2 + p^2}. \tag{34}$$

This result shows the exact relativistic dispersion relation and indicates that the nucleon's rest mass in the vacuum without a chiral condensate is given by $m_0 = 2.0589$ GeV, which is very larger than the real nucleon's mass. However, as will be shown, the chiral condensation can reduce this large mass to the real one.

Now, let us consider the effects of the current quark mass and the chiral condensate. The current quark mass breaks the chiral symmetry explicitly, while the chiral condensation breaks it spontaneously. To distinguish those two effects, let us first turn on the current quark mass without the chiral condensate, $m_q \neq 0$ and $\sigma = 0$. Then, the previous relativistic dispersion relation is slightly modified into

$$\omega^2 = m_0^2 + \left(p + g_Y m_q\right)^2. \tag{35}$$

In the $p = 0$ limit, the current quark mass slightly changes the nucleon's mass into $m^2 = m_0^2 + g_Y^2 m_q^2$. In the large momentum limit where $p \gg g_Y m_q$, however, the modified dispersion relation still remains as the relativistic one, $\omega \sim p$. It was shown that the meson's dispersion relation, regardless of m_q and σ, follows the similar relativistic form in the high momentum region [29].

If the chiral condensate is also turned on, the nucleon's dispersion relation is totally changed even in the vacuum. In Fig. 1(b), the nucleon's dispersion relation in the vacuum with a chiral condensate is depicted. Intriguingly, the obtained dispersion relation is well fitted by

$$\omega = 0.9390 + 0.97\, p^{0.979}. \tag{36}$$

As shown in this result, the chiral condensate dramatically reduces the nucleon's mass to the real mass of nucleons, from 2.0589 GeV to 0.9390 GeV. Another interesting point is that the chiral condensate modifies the momentum dependence in the small momentum limit, from p^2 to $p^{0.979}$. This is the story in vacuum with $Q = D = 0$, where there is no distinct between proton and neutron due to the absence of the isospin interaction.

3.2. Nucleon's rest mass in the nuclear medium

Now, let us consider nucleons in the nuclear medium. As shown in the previous section, the chiral condensate plays a crucial role in determining the nucleon spectrum so that from now on we focus on the case with $m_q = 2.38$ MeV, $\sigma = (304 \text{ MeV})^3$ and $g_Y = 4.699$. The rest masses of nucleons are determined from the energy in the zero momentum limit. In order see the nuclear density effect on the nucleon mass, we first turn off the isospin interaction by taking $D = 0$ but $Q \neq 0$. In this case, because of absence of the isospin interaction with the nuclear medium, proton and neutron are still degenerate. In Fig. 2(a), we plot the nucleon's rest mass depending on the nuclear density. In the low density regime below a certain critical density, the nucleon mass slowly decreases with increasing nuclear density, whereas it rapidly increases in the high density region.

In general cases with a nontrivial isospin interaction, masses of proton and nucleon are splitted and become non-degenerate like

the meson's spectra [28,29]. For $D = Q/2$ which describes the nuclear medium composed of 75% protons and 25% neutrons, the density dependence of nucleon's mass is depicted in Fig. 2(b). In the high density regime, the proton mass increases more rapidly than the neutron mass. In the high density regime the isospin interaction prefers creation of neutron rather than proton because in the nuclear medium with the positive net isospin charge more energy cost is required to create proton as expected. In the low density region, the proton mass decreases slightly faster than the neutron mass unlike the high density case. Another intriguing result is that nucleon has the lowest mass not at the zero density but at a certain critical density.

3.3. Dispersion relations

In the nonzero momentum limit, as mentioned before, the energy of the nucleon should be related to its momentum in order to satisfy the dispersion relation. This dispersion relation usually includes information for the interaction between nucleon and the background nuclear matter. In this section, after solving (29) and (30) with a nonzero momentum, we investigate effects of the nuclear density and the isospin interaction on the nucleon's dispersion relations. To do so, it should be noted that, when we describe the nuclear medium in the confining phase, there exists an upper bound in Q. For example, the deconfinement phase transition occurs at the critical value Q_c, $Q_c = 0.1679$ for $\alpha = 1/2$ and $Q_c = 0.1615$ for $\alpha = 1$ [28]. Therefore, we should restrict the range of Q to $0 \leq Q < Q_c$ for representing the confining phase. First, we pick up $Q = 0.1$ and $\alpha = 0$ to see only the nuclear density effect. In this case, since $D = 0$, there is no distinction between proton and neutron. The effect of the nuclear density on the nucleon's dispersion relation is plotted in Fig. 3(a), where the background nuclear density uplifts the nucleon's energy. In the small momentum limit, the dispersion relation is fitted by an almost linear curve

$$\omega = 0.9695 + 1.650\, p^{0.999}, \tag{37}$$

where 0.9695 GeV is the rest mass of nucleon at $Q = 0.1$ and $D = 0$. Fig. 3(b) shows the splitting of the nucleon's energy when we turn on $\alpha = 1/2$ with $Q = 0.1$. Similar to the meson case [28,29], the isospin interaction breaks the degeneracy of nucleons. Comparing it with Fig. 3(a), the isospin interaction increases the proton energy slightly, whereas the neutron's energy decreases.

4. Discussion

In this letter, we have studied the nucleon's rest mass and dispersion relation in the nuclear medium by using the AdS/CFT correspondence. To describe the nuclear medium with the flavor symmetry of the dual QFT, we introduced bulk gauge fields of $U(1)_L^2 \times U(1)_R^2 \subset U(2)_L \times U(2)_R$. These bulk gauge fields are dual to the quark number and isospin operator. In the confining phase, since nucleons rather than quarks are fundamental, we rewrote bulk gauge fields in terms of nucleon quantities by using the conservation of the net quark number, which uniquely determine the component ratio of proton and neutron in the nuclear medium.

On this background, we turned on the 5-dimensional fermionic fluctuations with mass, $\pm 5/2$, and reinterpreted them as 4-dimensional nucleons, which satisfy the 5-dimensional Dirac equation together with appropriate two boundary conditions. By solving the Dirac equation numerically, we have investigated rest masses and dispersion relations of the lowest parity-even states, proton and neutron. We found that the chiral condensate is crucial to explain the nucleon's rest mass because it dramatically changes the dispersion relation of nucleons unlike meson's spectra studied in [29].
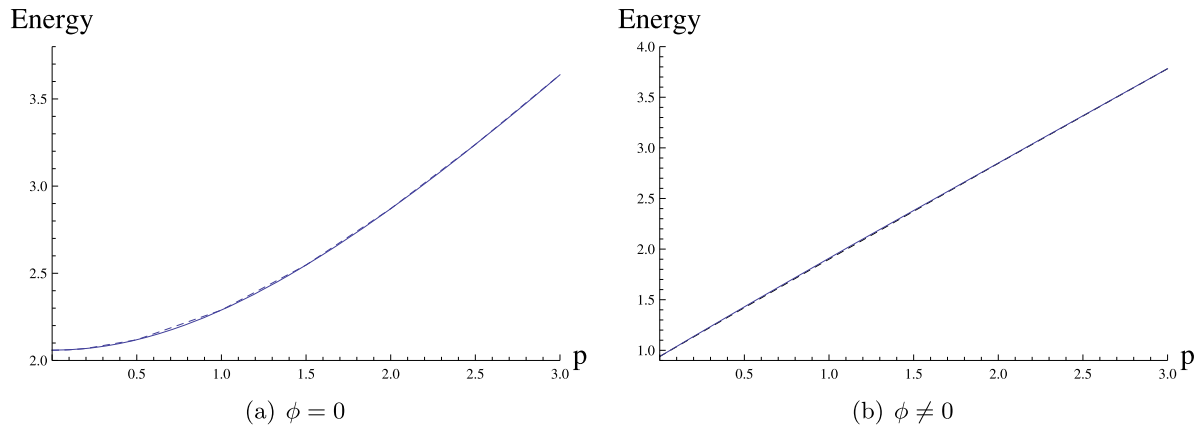
Fig. 1. The nucleon's mass in the vacuum (a) for $m_q = \sigma = 0$ and (b) with $m_q = 2.38$ MeV, $\sigma = (304 \text{ MeV})^3$ and $g_Y = 4.699$ which reproduce the correct nucleon's mass in the vacuum.
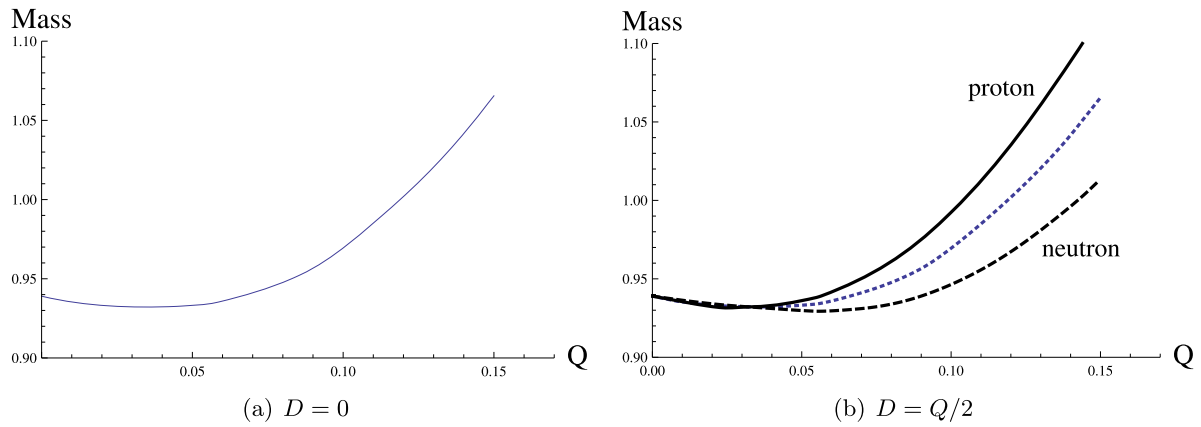
Fig. 2. The nucleon's mass spectrum in the nuclear medium. (a) For $D = 0$, proton and neutron are degenerate. (b) For $D = Q/2$, the masses of proton and neutron are splitted due to the isospin interaction, where the dotted line denotes the nucleon mass for $D = 0$.
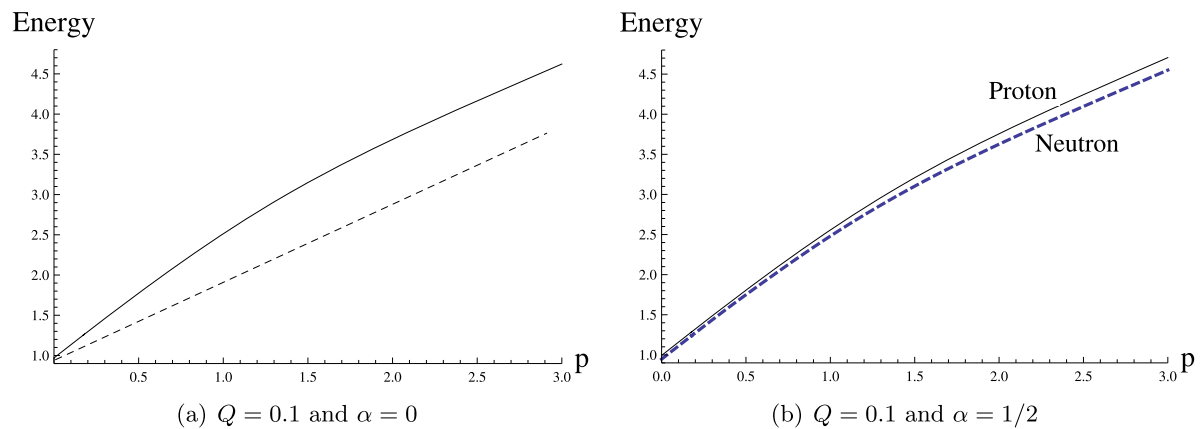
Fig. 3. The nucleon's dispersion relation in the nuclear medium. (a) The dashed and solid line indicate the dispersion relations in the vacuum and in the nuclear medium with the chiral condensate respectively. (b) The isospin interaction splits the degeneracy of nucleons. The energy of proton (neutron) slightly increases (decreases).

We also showed that in the high nuclear density regime, as expected, nucleon's rest mass increases with nuclear density, while in the low density regime it decreases unexpectedly. It would be interesting to figure out why such an unexpected nucleon's mass spectrum occurs in the low density regime.

We also showed that the number asymmetry between proton and neutron causes the mass and energy splitting between proton and neutron, which are similar to the meson mass splitting in the nuclear medium [28] and to the nucleon mass splitting in the isospin medium [39]. In the nuclear medium with the relative abundances of protons, the isospin interactions makes the proton's rest mass and energy become larger than those of neutron. These results would be helpful to understand nucleons in the nuclear medium quantitatively and qualitatively because there is no QFT tools applicable in the strong coupling regime.

Acknowledgements

References

[1] J.M. Maldacena, Adv. Theor. Math. Phys. 2 (1998) 231, arXiv:hep-th/9711200.
[2] S.S. Gubser, I.R. Klebanov, A.M. Polyakov, Phys. Lett. B 428 (1998) 105, arXiv:hep-th/9802109.
[3] E. Witten, Adv. Theor. Math. Phys. 2 (1998) 253, arXiv:hep-th/9802150.
[4] E. Witten, Adv. Theor. Math. Phys. 2 (1998) 505, arXiv:hep-th/9803131.
[5] O. Aharony, S.S. Gubser, J.M. Maldacena, H. Ooguri, Y. Oz, Phys. Rep. 323 (2000) 183, arXiv:hep-th/9905111.
[6] I.R. Klebanov, arXiv:hep-th/0009139.
[7] G.T. Horowitz, J. Polchinski, in: D. Oriti (Ed.), Approaches to Quantum Gravity, Cambridge University Press, 2009, pp. 169–186, arXiv:gr-qc/0602037.
[8] J. Erlich, E. Katz, D.T. Son, M.A. Stephanov, Phys. Rev. Lett. 95 (2005) 261602, arXiv:hep-ph/0501128.
[9] L. Da Rold, A. Pomarol, Nucl. Phys. B 721 (2005) 79, arXiv:hep-ph/0501218.
[10] A. Karch, E. Katz, D.T. Son, M.A. Stephanov, Phys. Rev. D 74 (2006) 015005, arXiv:hep-ph/0602229.
[11] T. Sakai, S. Sugimoto, Prog. Theor. Phys. 113 (2005) 843, arXiv:hep-th/0412141.
[12] T. Sakai, S. Sugimoto, Prog. Theor. Phys. 114 (2005) 1083, arXiv:hep-th/0507073.
[13] J.M. Maldacena, Phys. Rev. Lett. 80 (1998) 4859, arXiv:hep-th/9803002.
[14] S.J. Rey, J.T. Yee, Eur. Phys. J. C 22 (2001) 379, arXiv:hep-th/9803001.
[15] C. Park, Phys. Rev. D 81 (2010) 045009, arXiv:0907.0064 [hep-ph].
[16] C.P. Herzog, Phys. Rev. Lett. 98 (2007) 091601, arXiv:hep-th/0608151.
[17] K.B. Fadafan, E. Azimfard, Nucl. Phys. B 863 (2012) 347, arXiv:1203.3942 [hep-th].
[18] S. Nakamura, Y. Seo, S.J. Sin, K.P. Yogendran, J. Korean Phys. Soc. 52 (2008) 1734, arXiv:hep-th/0611021.
[19] S. Nakamura, Y. Seo, S.J. Sin, K.P. Yogendran, Prog. Theor. Phys. 120 (2008) 51, arXiv:0708.2818 [hep-th].
[20] S.K. Domokos, J.A. Harvey, Phys. Rev. Lett. 99 (2007) 141602, arXiv:0704.1604 [hep-ph].
[21] B.-H. Lee, C. Park, S.J. Sin, J. High Energy Phys. 0907 (2009) 087, arXiv:0905.2800 [hep-th].
[22] K. Jo, B.-H. Lee, C. Park, S.J. Sin, J. High Energy Phys. 1006 (2010) 022, arXiv:0909.3914 [hep-ph].
[23] Y. Kim, Y. Seo, I.J. Shin, S.J. Sin, J. High Energy Phys. 1106 (2011) 011, arXiv:1011.0868 [hep-ph].
[24] P. Colangelo, F. Giannuzzi, S. Nicotri, Phys. Rev. D 83 (2011) 035015, arXiv:1008.3116 [hep-ph].
[25] R.G. Cai, S. He, D. Li, J. High Energy Phys. 1203 (2012) 033, arXiv:1201.0820 [hep-th].
[26] P. Colangelo, F. Giannuzzi, S. Nicotri, J. High Energy Phys. 1205 (2012) 076, arXiv:1201.1564 [hep-ph].
[27] C. Park, Phys. Lett. B 708 (2012) 324, arXiv:1112.0386 [hep-th].
[28] B.-H. Lee, S. Mamedov, S. Nam, C. Park, J. High Energy Phys. 1308 (2013) 045, arXiv:1305.7281 [hep-th].
[29] B.-H. Lee, C. Park, S. Nam, arXiv:1412.3097 [hep-ph].
[30] D. Albrecht, J. Erlich, Phys. Rev. D 82 (2010) 095002, arXiv:1007.3431 [hep-ph].
[31] H. Nishihara, M. Harada, Phys. Rev. D 89 (7) (2014) 076001, arXiv:1401.2928 [hep-ph].
[32] H. Nishihara, M. Harada, Phys. Rev. D 90 (11) (2014) 115027, arXiv:1407.7344 [hep-ph].
[33] D.K. Hong, T. Inami, H.-U. Yee, Phys. Lett. B 646 (2007) 165, arXiv:hep-ph/0609170.
[34] D.K. Hong, M. Rho, H.U. Yee, P. Yi, Phys. Rev. D 76 (2007) 061901, arXiv:hep-th/0701276 [hep-th].
[35] D.K. Hong, M. Rho, H.U. Yee, P. Yi, J. High Energy Phys. 0709 (2007) 063, arXiv:0705.2632 [hep-th].
[36] H.C. Kim, Y. Kim, U. Yakhshiev, J. High Energy Phys. 0911 (2009) 034, arXiv:0908.3466 [hep-ph].
[37] H.C. Ahn, D.K. Hong, C. Park, S. Siwach, Phys. Rev. D 80 (2009) 054001, arXiv:0904.3731 [hep-ph].
[38] P. Zhang, Phys. Rev. D 81 (2010) 114029, arXiv:1002.4352 [hep-ph].
[39] B.-H. Lee, S. Mamedov, C. Park, Int. J. Mod. Phys. A 29 (29) (2014) 1450170, arXiv:1402.6061 [hep-ph].
[40] M. Henningson, K. Sfetsos, Phys. Lett. B 431 (1998) 63, arXiv:hep-th/9803251.
[41] W. Mueck, K.S. Viswanathan, Phys. Rev. D 58 (1998) 041901, arXiv:hep-th/9804035.
[42] M. Henneaux, in: International Meeting on Mathematical Methods in Modern Theoretical Physics, ISPM 98, Tbilisi, 1998, pp. 161–170, arXiv:hep-th/9902137.
[43] R. Contino, A. Pomarol, J. High Energy Phys. 0411 (2004) 058, arXiv:hep-th/0406257.
[44] B.-H. Lee, C. Park, S. Shin, J. High Energy Phys. 1012 (2010) 071, arXiv:1010.1109 [hep-th].